Astronomy reports

Each year approximately 200 different proposals are allocated time to conduct astronomical research programs on ATNF facilities. This chapter describes a few of the astronomy highlights from the year.

The first double pulsar

R. N. Manchester on behalf of the Parkes High-Latitude Pulsar Survey team: M. Burgay (University of Bologna, Italy); F. Camilo (Columbia University, USA); N. D'Amico (Cagliari Astronomical Observatory, Italy); P. C. C. Freire (Arecibo Observatory, Puerto Rico); B. C. Joshi (GMRT, India); M. Kramer (University of Manchester, UK); D. R. Lorimer (University of Manchester, UK); A. G. Lyne (University of Manchester, UK); M. A. McLaughlin (University of Manchester, UK); R. N. Manchester (ATNF); A. Possenti (Cagliari Astronomical Observatory, Italy); J. Reynolds (ATNF) and J. Sarkissian (ATNF)

Pulsars have a history of new and unexpected developments – think of the first period glitch, the first binary pulsar and the first millisecond pulsar. These and other similar discoveries have had profound and wide-ranging implications, impacting not only on pulsar astrophysics, but also on stellar evolution, gravitational physics, astrometry and many other areas. This tradition has continued with the discovery of the first-known double-pulsar system at Parkes. Beginning with the famous Hulse-Taylor binary pulsar (PSR B1913+16), it has been known for a long time that in some binary systems the companion, as well as the pulsar, is a neutron star. Only five or six of the 80 or so previously known binary pulsars are believed to be double-neutron-star systems and, despite careful searches, in no case had the second neutron star been detected as a pulsar. This is not too surprising as the second-born pulsar has a much shorter lifetime than the first, which in all known systems has been "recycled" to form a rapidly spinning and weakly magnetised pulsar.

This story begins with the discovery of a 22-millisecond pulsar, PSR J0737–3039, by Marta Burgay, a University of Bologna student working with the Parkes High-Latitude Pulsar Survey team. This survey uses the Parkes multibeam receiver to search a region of sky in the third Galactic quadrant extending between latitudes of –60° and +60°. It was immediately clear that PSR J0737–3039 was a member of a binary system, which subsequent observations showed to have a period of only 2.4 hours. Furthermore, the amplitude of the Doppler shifts showed that the companion was massive and probably another neutron star. With a mean orbital velocity of 0.1 per cent of the velocity of light, this is the most relativistic binary pulsar known and many relativistic perturbations of the observed pulsar period are expected to be detectable. Indeed, the relativistic precession of periastron was observed in just a few days, implying that the sum of the masses of the two stars is about 2.59 solar masses. One of the most interesting aspects of this system is that it raises the predicted rate of detections of double-neutron-star mergers by gravitational wave detectors such as LIGO by nearly an order of magnitude. These results were published in Nature by Burgay et al. in December 2003. Figure 13 shows an artist's impression of the two pulsars.

These results were very exciting, but this system had more surprises in store. While testing a pulsar search program on a Parkes observation of this pulsar, Duncan Lorimer was astounded to see a very strong signal at a period of 2.78 s with a dispersion measure equal to that of the 22-ms pulsar. Further investigation showed that this signal had the inverted Doppler shifts of the 22-ms pulsar. There was no doubt that it was the neutron-star companion – the first time that the second neutron star in such a system had been seen as a pulsar! The emission from this pulsar, PSR J0737–3039B, is strongly modulated with orbital phase and only bright for two 10-minute intervals during the 2.4-hour orbit. At the time of the discovery-observation of the A pulsar, the B pulsar was turned off! The discovery of the B pulsar was announced in Science Express on 8 January 2004 and published in Science in the 20 February 2004 issue (Lyne et al. 2004).

Figure 14 shows the orbital modulation of the B pulsar signal. This figure shows that not only is the pulse amplitude varying with orbital phase, the pulse shape is also changing! Such modulation is unprecedented in pulsar astronomy, and is very likely due to the relativistic wind from the A pulsar penetrating deep into the magnetosphere of the B pulsar. Back-of-the-envelope calculations suggest that more than 90 per cent of the B-pulsar magnetosphere is actually blown away by the A-pulsar wind – it is amazing that the B pulsar can pulse at all!

It has also been possible to observe an eclipse of the A-pulsar signal as it passes behind the B pulsar. It turns out that the binary system is seen almost edge-on, another very fortuitous circumstance. The most direct evidence for

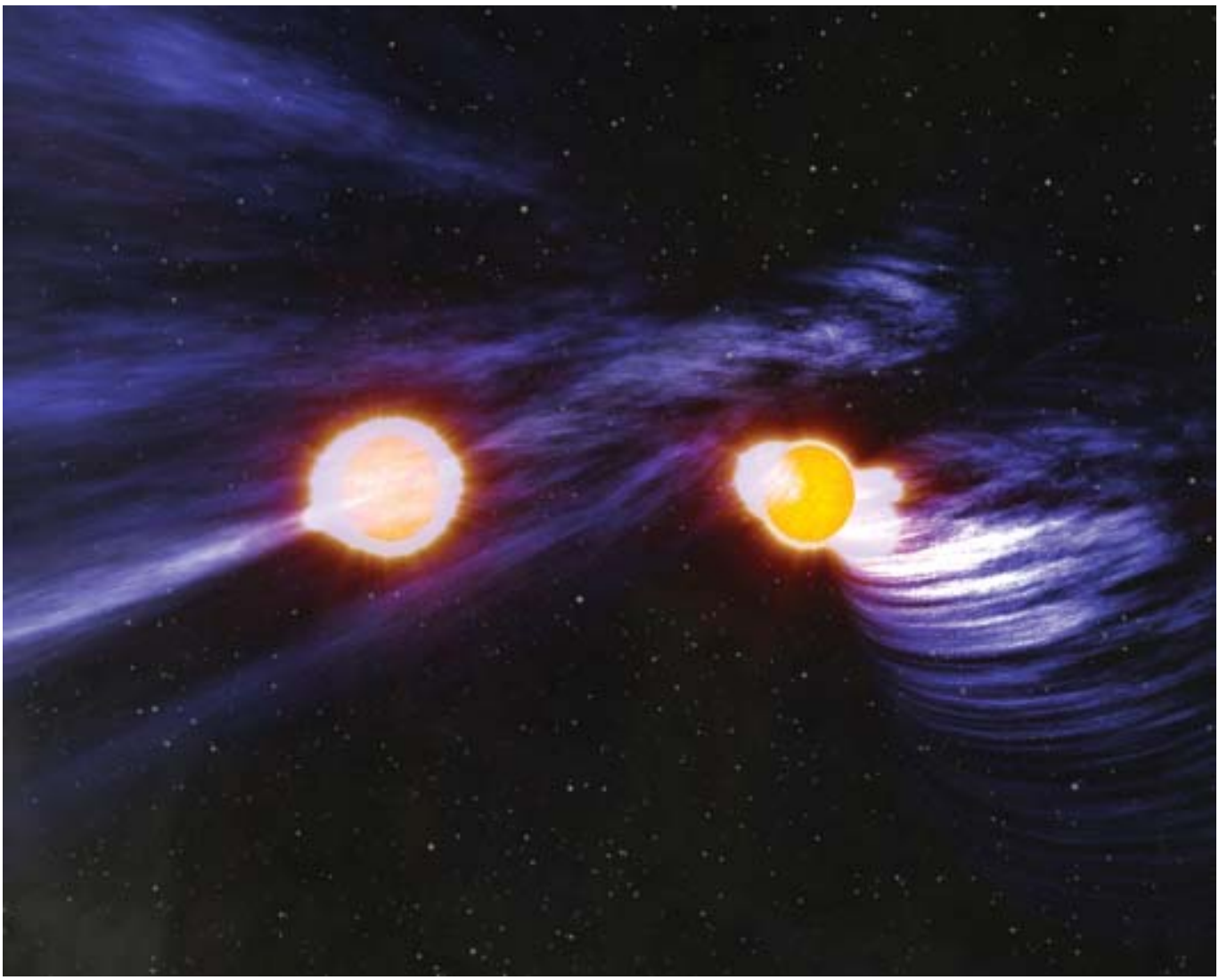

Figure 13 An artist's impression of the two pulsars orbiting around the common centre of mass. The faster rotating pulsar spins almost 3000 times a minute while the slower rotating pulsar spins only 22 times a minute. The two pulsars orbit each other once every 2.4 hours.
Image credit: John Rowe Animation

this is the detection of the so-called "Shapiro delay" in the A-pulsar signal resulting from deflection of the ray path as it passes near the companion. This has an amplitude of about 100 microseconds, implying that the orbit plane is within three degrees of being edge-on. The A eclipse is very short, lasting about 30 seconds, a duration roughly consistent with occultation by the remaining part of the B-pulsar magnetosphere.

Detection of the second neutron star as a pulsar opens up a whole new set of investigations in relativistic gravity. The ratio of the orbital Doppler shifts immediately gives the mass ratio of the two stars. Importantly, this ratio is largely independent of theories of gravity and hence it provides an important constraint on such theories. As Figure 15 shows, the mass-ratio and periastron-advance constraints are nearly orthogonal and hence accurately determine the two neutron-star masses: 1.337 +/- 0.004 solar masses and 1.251 +/- 0.004 solar masses. The three other relativistic constraints and the "mass function" constraint for the two stars are all consistent with these values, confirming the accuracy of predictions made by Einstein's general theory of relativity. In the next few years, we expect to measure several more relativistic effects, some dependent on higher-order terms in the post-Newtonian expansion. These will provide the tightest constraints yet on theories of gravity in the strong-field regime.

References:

Burgay, M., D'Amico, N., Possenti, A., Manchester, R.N., Lyne, A.G., Joshi, B.C., McLaughlin, M.A., Kramer, M., Sarkissian, J. M. Camilo, F., Kalogera, V., Kim, C, & Lorimer, D.R., 2003, Nature, 426, 531-533.

Lyne, A.G., Burgay, M., Kramer, M., Possenti, A, Manchester, R.N., Camilo, F., McLaughlin, M.A., Lorimer, D.R., D'Amico, N., Joshi, B.C., Reynolds, J.E. & Freire, P.C.C., 2004, Science, 303, 1153-1157.

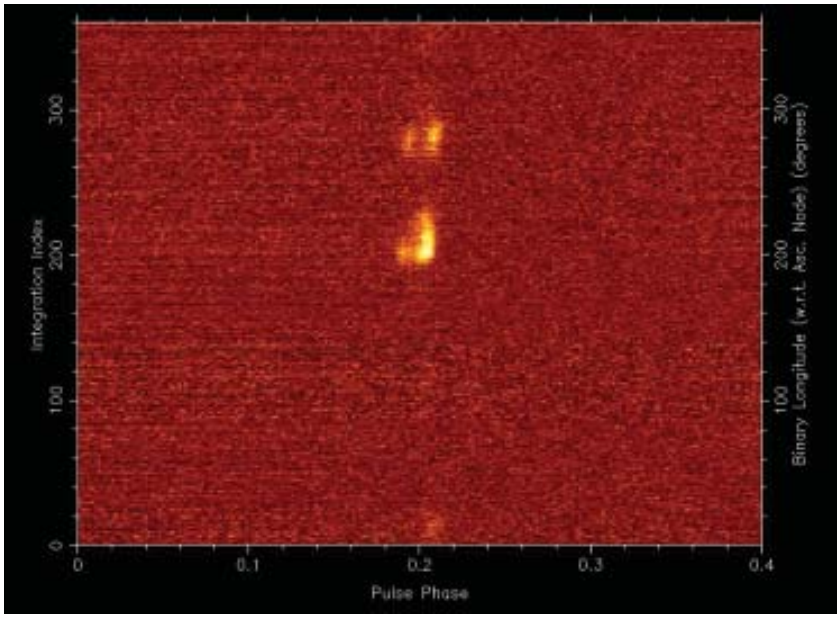

Figure 14 Intensity of PSR J0737-3039B at 3.1 GHz as a function of pulse phase and true orbital longitude. Approximately 40 per cent of the pulse period is displayed. Longitude 270° corresponds to inferior conjunction of the B pulsar when it is in front of and most closely aligned with the A pulsar. About 13.7 hours of data were averaged to form this image. The data were obtained with the recently commissioned Parkes 10/50cm receiver and analysed using the PSRCHIVE pulsar analysis package.

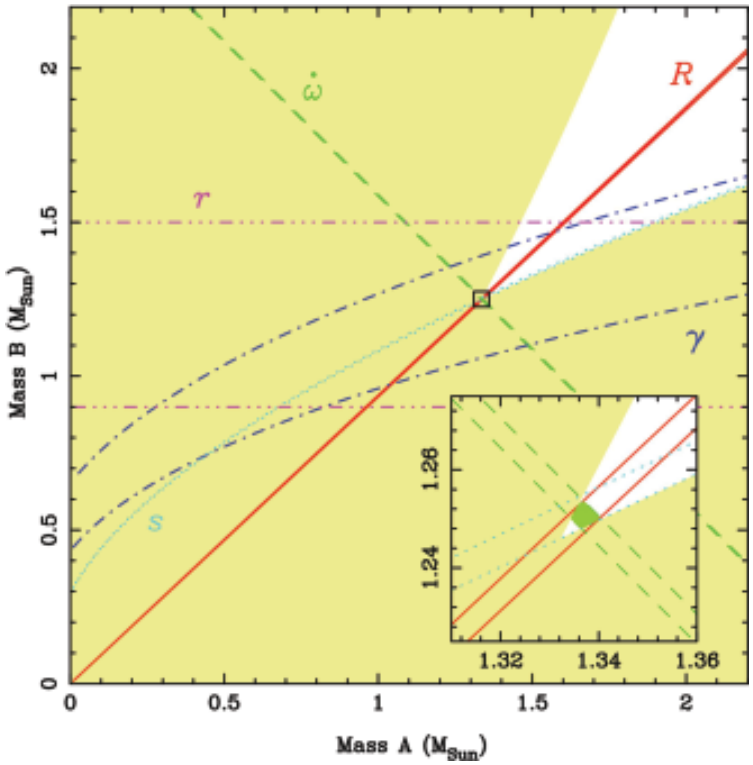

Figure 15 Constraints on the masses of the two neutron stars in the PSR J0737-3039A/B system. The yellow regions are forbidden by the constraint that the sine of the orbit inclination angle cannot exceed unity. The solid diagonal lines (marked *R*) define the limits on the mass ratio. Additional constraints are provided by the detection of relativistic effects in the timing of the A pulsar, interpreted in the framework of general relativity. The diagonal dashed lines are limits on the sum of the masses based on the observed precession of periastron and the dot-dash lines are limits based on variations in time dilation as the pulsar moves around its somewhat eccentric orbit. The other two constraints, marked *r* and *s*, are based on the observed Shapiro delay. The inset shows an expanded plot of the region of intersection of the various constraints. (Lyne et al. 2004)

Temperature maps of dense molecular gas in starburst galaxies

J. Ott (ATNF); A. Weiss (Instituto de Radioastronomía Milimétrica; Spain); C. Henkel (Max Planck Institut fûr Radioastronomie, Germany); F. Walter (National Radio Astronomy Observatory, USA)

The new 12-mm receiver system (installed at the Compact Array in April 2003) allows astronomers, for the first time, to perform interferometric observations in the southern hemisphere in this important frequency range. Within this band lie the lowest transitions of the abundant ammonia (NH_3) molecule. The specific tetrahedral structure of ammonia and the resulting metastable inversion lines can be used as an excellent thermometer of cold, dense, molecular gas - the material from which stars ultimately form. In an ongoing project, Ott and his collaborators are using this tool to compute temperature maps of the molecular cores of nearby starburst galaxies at the very high spectral and angular resolution provided by the Compact Array.

Starburst galaxies exhibit current star formation rates of tens, and in extreme cases up to hundreds, of solar masses per year. The subsequent release of mechanical energy from massive stars, in the form of strong stellar winds and numerous supernova explosions, heats the ambient gas and drives superwinds perpendicular to the gaseous and stellar disks. The ionised material of superwinds can be traced by optical spectral lines and X-ray line and continuum emission at distances of up to tens of kiloparsecs from the galaxies themselves. The fuel for these periods of extreme star formation is provided by molecular gas which is found abundantly in the starburst cores.

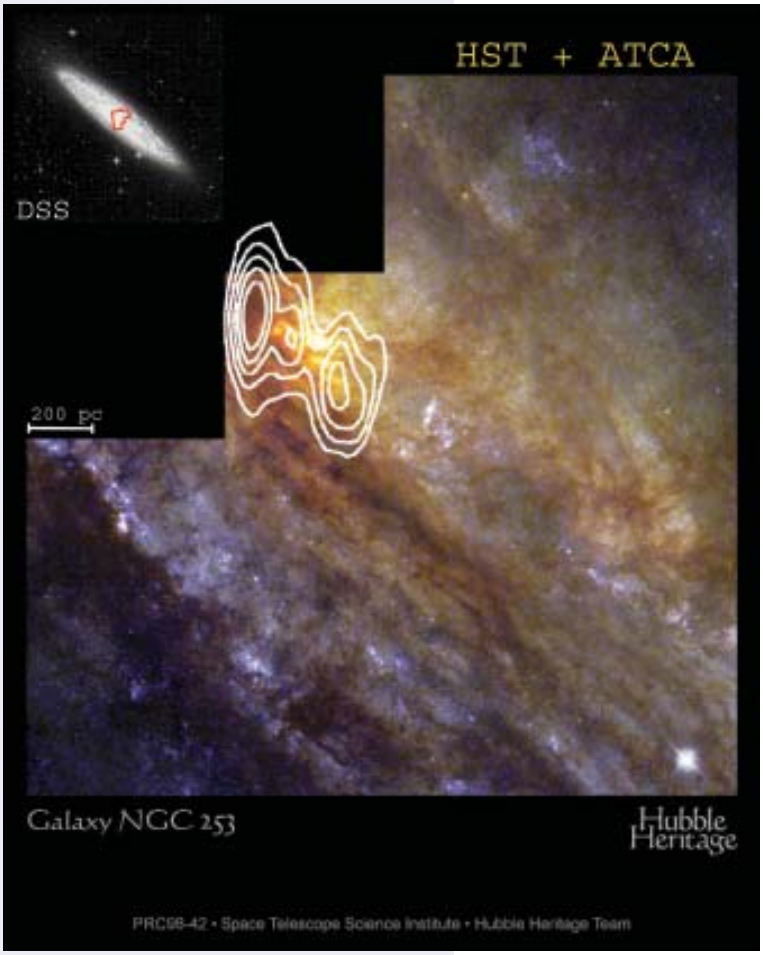

Figure 16 A Hubble Heritage Image of NGC 253. Overlaid as contours are the Compact Array observations of the NH_3 (1,1) inversion line. This traces cold and dense molecular gas that feeds a starburst region in the centre of the galaxy. The orientation and coverage of the "batwing-shaped" Hubble Space Telescope WFPC2 instrument for this observation is marked on top of the Digitized Sky Survey image of NGC 253 shown in the upper left corner. Note that the image is rotated by approximately 180° compared to the representations in Figures 17 and 19.

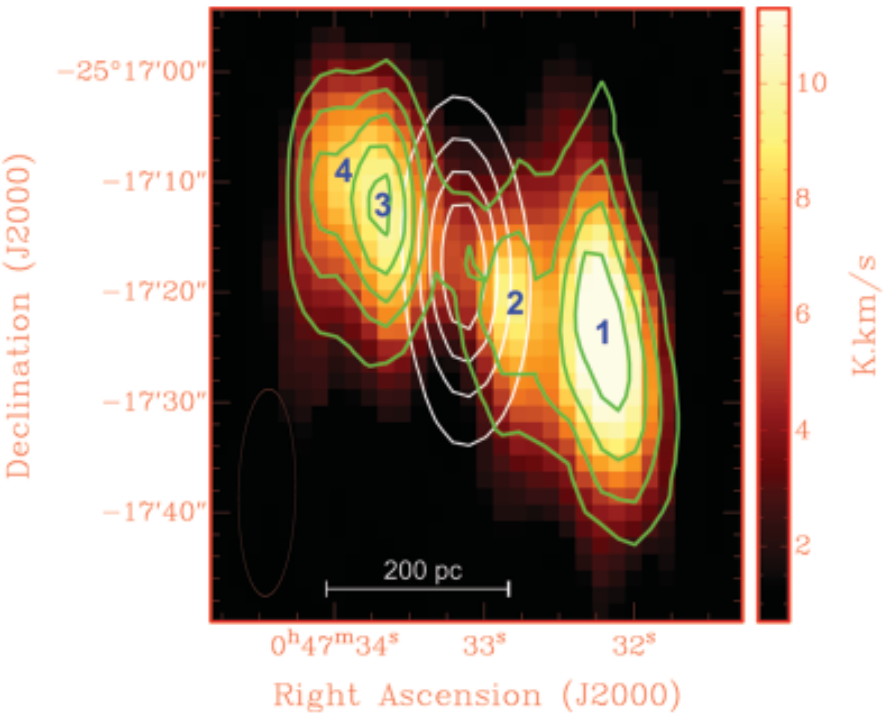

Figure 17 Maps of the ammonia (1,1) (image) and (2,2) (green contours) inversion lines toward NGC 253. The 12-mm continuum emission, which marks the high star formation rate in the nucleus, is shown as white contours. Clumps 1 – 4 are marked by numbers. The size of the synthesised beam is shown in the lower left corner.

NGC 253 is a prominent, nearby starburst galaxy. Located at a distance of only 2.6 million parsecs, it exhibits a current star formation rate of five solar masses per year, of which 3.5 solar masses per year are concentrated in the central 200 parsecs (Figure 16). This region is surrounded by vast amounts of molecular gas (30 million solar masses) and the densest parts of it (volume densities $>10^4$ cm^{-3}) are traced by ammonia. The brightest NH_3 emission is observed at both sides of the starburst centre decreasing toward the centre itself and toward radii larger than about 200 parsecs (Figure 17). The high angular and spectral resolution of the Compact Array allows the identification of four dense molecular complexes, two on each side of the starburst core (Figures 17 and 18). The dynamics of the clumps are quite complex as is illustrated by the position-velocity diagram displayed in Figure 18. Simple models such as a ring rotating like a solid body are not in agreement with the data.

Figure 19 shows a rotational temperature map of the dense molecular gas, calculated using the relative strengths of the NH_3 (1,1) and (2,2) inversion lines. The temperature distribution is surprisingly variable ranging from approximately 30 Kelvin close to the starburst centre and 35 Kelvin in the south-western complexes to about 60 Kelvin in the north-eastern molecular clouds. The gas temperatures and radial temperature gradients are different on opposite sides of the starburst centre. Clump 2 is probably the closest molecular complex to the starburst centre (Figure 18) and it is surprising that this cloud has the lowest temperature. It appears that heating by the weak active galactic nucleus (AGN) or by the nuclear starburst does not dominate the heating processes in the molecular clouds. Instead, cloud 2 may be the first of the four complexes to be converted into stars and to support starburst activity.

While temperatures are not consistent with a systematic trend as a function of galactocentric radius, abundances do show such a trend. The ratio of ammonia to molecular hydrogen, NH_3 /H_2, is about 5.5 x 10^{-9} in the outer molecular complexes; the central diffuse region between clouds 2 and 3 exhibits a relative abundance of only about 2.5x10^{-9}. This effect can be explained by the strong UV radiation of the star-forming region near cloud 2 which destroys ammonia in its vicinity. Alternatively, the high densities required for the excitation of ammonia

might only be largely met in the molecular complexes but not in the more diffuse, central volume. The faint molecular gas component observed at the very starburst centre might therefore be part of the debris after preceding dense components collapsed into stars.

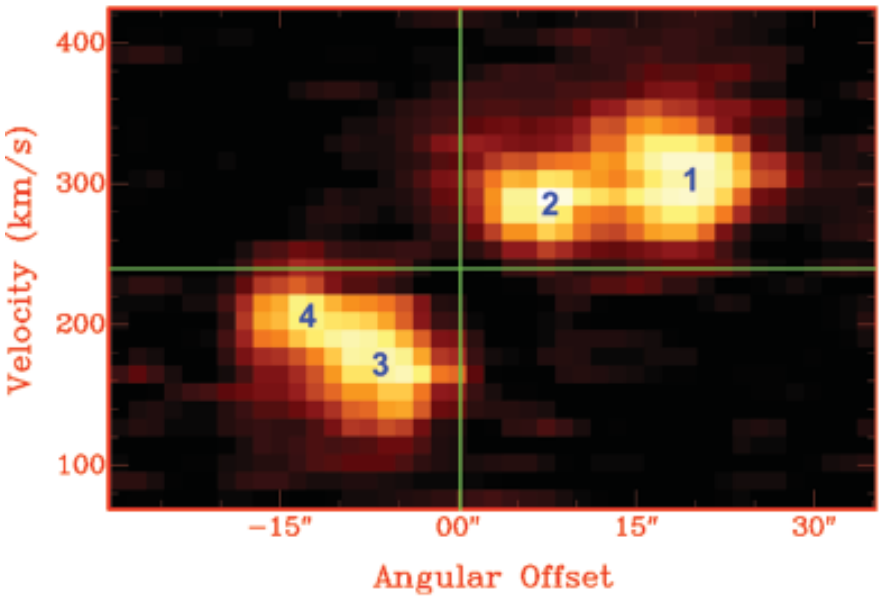

Figure 18 A position-velocity diagram showing the ammonia (1,1) emission along the minor axis of NGC 253. The green lines indicate the starburst centre in terms of position and systemic velocity. The angular offset increases toward the south-west. Individual molecular complexes are numbered as in Figure 17.

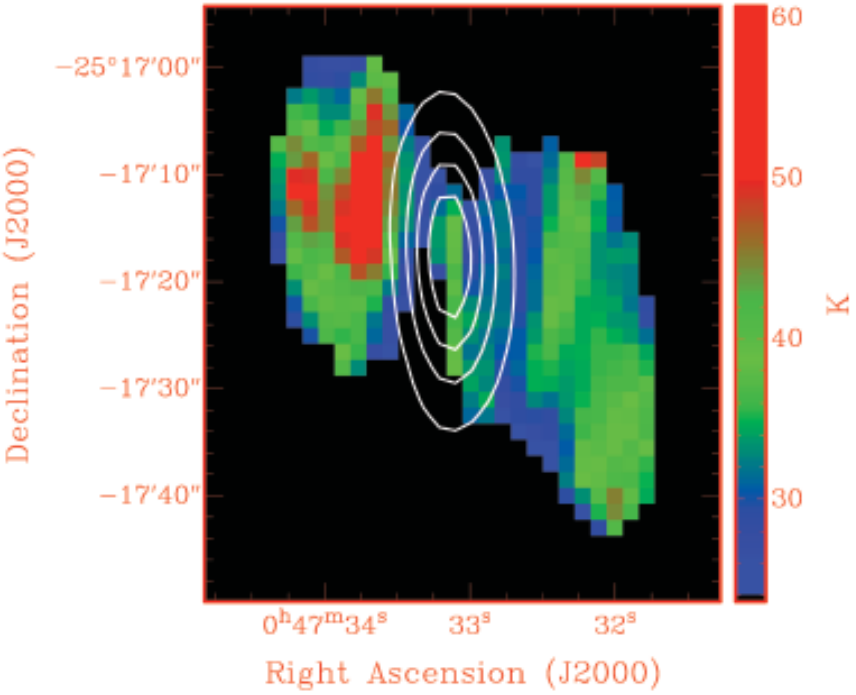

Figure 19 A rotational temperature map of the dense, cold molecular gas. This map is derived using the line ratio of the ammonia (1,1) and (2,2) transitions. The starburst centre is indicated by the 12-mm continuum emission (white contours). Note that the temperature varies by a factor of about 2 from 35 Kelvin in the south-west to 60 Kelvin toward the north-east. The lowest temperatures of around 30 Kelvin are observed at the starburst centre. This image is on the same scale as Figure 17.

What and where are the High-Velocity Clouds around the Milky Way?

D.J. Pisano (ATNF); Brad Gibson (Swinburne University of Technology); David Barnes (University of Melbourne); Lister Staveley-Smith (ATNF); Ken Freeman (Research School of Astronomy and Astrophysics, Australian National University); Virginia Kilborn (Swinburne University of Technology/ATNF)

Over 40 years ago, astronomers discovered clouds of neutral hydrogen (HI) around the Milky Way moving at velocities inconsistent with Galactic rotation; these clouds were termed "high-velocity clouds" or HVCs. Because HVCs are not in simple Galactic rotation and have no associated stars, it has been impossible to determine their distances and, hence, their masses. Without such basic information, astronomers have been limited to indirect methods to infer the origin of HVCs. Today, it appears that a variety of processes can explain the origin of HVCs, and that they, perhaps, reside over a large range in distance.

Some HVCs are probably related to a Galactic fountain. A Galactic fountain occurs when a number of supernovae in the disk of our Galaxy explode in close proximity over a short period of time. The combined energy of the explosions lifts the interstellar gas into the halo of our Galaxy, where it cools and rains back onto the disk. In this scenario, HVCs are the cooling gas falling back onto our Galaxy, residing in the near Galactic halo, only tens of thousands of parsecs from the disk.

Some HVCs are certainly tidal in origin. The Magellanic Stream is the most prominent tidal feature in the sky, a tidal tail created by the interaction between the Large and Small Magellanic Clouds and the Milky Way. Because of its association with the Magellanic Clouds, the Stream is known to be located at a distance of approximately 55,000 parsecs. Other HVCs may be related to the accretion of the Sagittarius dwarf galaxy or other satellite galaxies by the Milky Way and would reside at similar distances.

One of the original ideas as to the nature of HVCs was that they are infalling primordial gas contributing to the formation of the Milky Way. These clouds would have low metallicities, having not been enriched by supernovae, and may be located either near or far from the Milky Way. At least one large HVC complex has a measured low metallicity and a distance of at least 5000 parsecs. The idea that HVCs reside at very large distances, about one million parsecs from the Milky Way, is nearly as old as the discovery of HVCs themselves. Originally, this idea was dismissed because their inferred HI masses would not be large enough for HVCs to be stable. Recently, this idea has undergone a refinement. Leo Blitz and collaborators, as well as Robert Braun and Butler Burton, have proposed that at least some of the HVCs are associated with dark matter halos and reside at distances of up to a million parsecs from the Milky Way, and contain of order 10 million solar masses of HI.

Current models of hierarchical galaxy formation predict that the Local Group should contain roughly 300 low mass, dark matter halos; an order of magnitude higher than the number of known luminous dwarf galaxies. This is commonly known as the "missing satellite" problem. If the HVCs reside within the excess dark matter halos, then the total number of HVCs and dwarf galaxies matches the predictions of simulations, thus solving the problem. In this case, HVCs are the building blocks for the continued assembly of the galaxies contained within the Local Group. This scenario is easily tested: if HVCs are associated with galaxy and group formation, then their analogues will be visible in other groups of galaxies similar to the Local Group. If no HVC analogues are detected, then limits on their masses and their distances can be inferred.

Over the past three years Pisano and his collaborators have been using the Parkes multibeam instrument to search for HVC analogues in six loose groups of galaxies similar to the Local Group in structure and morphology. A loose group is a collection of a few large galaxies and tens of smaller galaxies that are separated by a distance much larger than the size of individual galaxies and spread over a diameter of approximately one million parsecs. The groups observed contained only spiral galaxies, just like the Local Group. The observations were sensitive to clouds with HI masses down to 10 million solar masses. An example is shown in Figure 20, which shows a map of the total HI intensity in the LGG 93 group. All Parkes HI detections were confirmed with follow-up Compact Array observations which also provided better spatial resolution to search for optical counterparts. In the three groups for which the Parkes detections have been confirmed, ten new HI-rich dwarf galaxies were detected. An example of two of these dwarf galaxies is shown in Figure 21. The Compact Array observations had the same sensitivity as the Parkes data, so even if an HI cloud was unresolved by Parkes, it would have been detected with the Compact Array. Nevertheless, no HI clouds without stars, HVC analogues, were found in the three groups using either telescope.

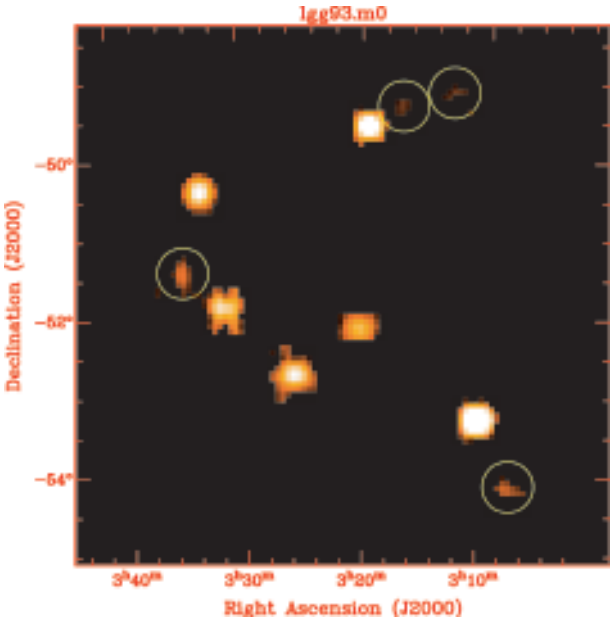

Figure 20 A total HI intensity map of the LGG 93 group obtained using Parkes multibeam data. The circles show the new detections of four dwarf galaxies.

The non-detection of HVC analogues in these three groups allows constraints to be placed on the masses of the clouds. If the HI clouds in the target groups have the same properties as the HVCs seen around the Milky Way, then a failure to detect them implies that the average HI mass of HVCs is less than 400,000 solar masses, and the clouds must be clustered within 160,000 parsecs of the Milky Way and the group galaxies. These limits are in good agreement with recent models and inferred distances to HVCs around the Milky Way made by other astronomers using a variety of different methods. They firmly rule out the original models of Blitz and collaborators and Braun & Burton, which place HVCs at a distance of one million parsecs. It does not mean that HVCs lack dark matter, but only that they are tightly clustered around galaxies and contain much less mass than these authors originally believed.

Overall, this has profound implications for the importance of HVCs in the Local Group. Namely, the total HI mass in HVCs is less than 100 million solar masses; roughly equivalent to a single gas-rich dwarf galaxy. As such, there is very little neutral matter in HVCs present in the selected groups or the Local Group that is available for accretion by the large galaxies to fuel future star formation. Furthermore, because HVCs must be tightly clustered around the Milky Way, they are not so much associated with the formation of the Local Group, but more with the formation of individual galaxies if they do contain dark matter. Unfortunately, future searches for HVC analogues in other groups to further constrain their nature will be very difficult due to the extreme sensitivity required. These observations will probably have to wait for the next generation of radio telescopes.

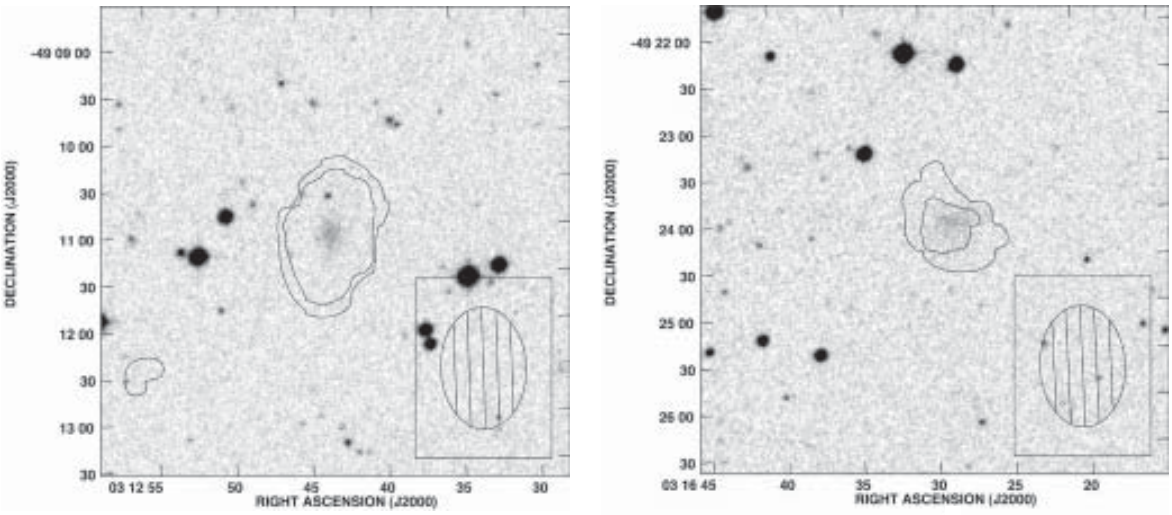

Figure 21 Two dwarf galaxies, LGG 93-1 (left) and LGG 93-2 (right), found in the Parkes multibeam survey. The contours represent the total HI intensity from the follow-up Compact Array observations. The grayscale is from the Digitized Sky Survey and illustrates that both HI detections contain stars and are, indeed, dwarf galaxies and not analogous to the high-velocity clouds. The hatched ovals represent the spatial resolution of the observations.

Gamma-ray burst jets in type Ib/c supernovae

A. M. Soderberg (California Institute of Technology, USA); D. A. Frail (National Radio Astronomy Observatory, USA) and M. H. Wieringa (ATNF)

As the most luminous objects in the Universe, gamma-ray bursts (GRBs) have grabbed the attention of both astronomers and the public. However, during the 31 years since the discovery of gamma-ray bursts, the nature and origin of these powerful collimated explosions has remained largely unknown. Recently, with the discovery of a relatively nearby gamma-ray burst event on 29 March 2003, known as GRB 030329, spectroscopic observations have provided undeniable evidence that long-duration gamma-ray bursts originate from supernovae (SNe) explosions that follow the end of nuclear burning and core collapse in massive stars.

The first important observational clue that there is a link between gamma-ray bursts and the deaths of massive stars came in April 1998. Responding to a new gamma-ray burst, GRB 980425, astronomers found to their surprise an ultra-luminous Type Ic supernova, SN 1998bw, coincident with the satellite position, but located a mere 40 million parsecs away! Based on Compact Array observations, SN 1998bw was shown to be an unusually energetic supernova with properties similar to those observed in cosmological gamma-ray bursts, thus bolstering the idea that the two explosive events were related. However, while the Compact Array observations strengthened the link between gamma-ray bursts and stellar death, it produced its own puzzle: What is the connection (if any) between GRB 980425 and the much more distant cosmological gamma-ray bursts?

Despite being the nearest burst detected to date, the "afterglow" emission from GRB 980425 was under-luminous compared to all other gamma-ray bursts. Afterglow emission is produced by particle acceleration within the collimated gamma-ray burst ejecta (jet) as it sweeps up and shocks the interstellar medium. During the six years since the event of GRB 980425 the radio afterglow has been monitored with the Compact Array (Kulkarni et al. 1998). The most recent measurements in, December 2003 by Soderberg and her colleagues, showed that the radio emission continues to decay as a power-law.

These recent data are of extreme importance in determining the relation between GRB 980425 and other gamma-ray bursts. One popular theory posits that GRB 980425/SN 1998bw was a typical gamma-ray burst viewed far away from the collimation axis of the jet. In this scenario, the afterglow emission is initially beamed away from us and therefore appears sub-luminous. However, as the gamma-ray burst jet decelerates it begins to spread sideways and eventually reaches spherical symmetry on a timescale of one to ten years, depending on the density of the surrounding medium. When the jet spreads into our line-of-sight it should produce a sharp rise in the observed radio afterglow emission. However, six years after the burst, the Compact Array observations do not show any evidence for a sharp rise in the radio emission and thus no evidence that GRB 980425 was initially pointed away from our line-of-sight. This result was combined with upper limits for 15 local (less than 100 million parsecs) type Ibc supernovae between one and 20 years old to show that at most six per cent of local SNe have associated gamma-ray burst jets.

An alternative to the off-axis jet hypothesis considers the event of GRB 980425/SN 1998bw as a member of a separate class of sub-energetic explosions characterised by fainter afterglow emission. This theory is supported by the recent event, GRB 031203, the nearest burst besides GRB 980425, which similarly showed a sub-luminous afterglow and association with an ultra-luminous type Ic supernova (SN 2003lw). With the launch of the NASA spacecraft SWIFT in late 2004, to search for gamma-ray burst events, it is anticipated that a significant population of similar local sub-energetic gamma-ray burst events will be revealed.

Figure 22 (page 28) A schematic representation of a gamma-ray burst.
Image credit: Dan Berry, Skyworks Digital, USA

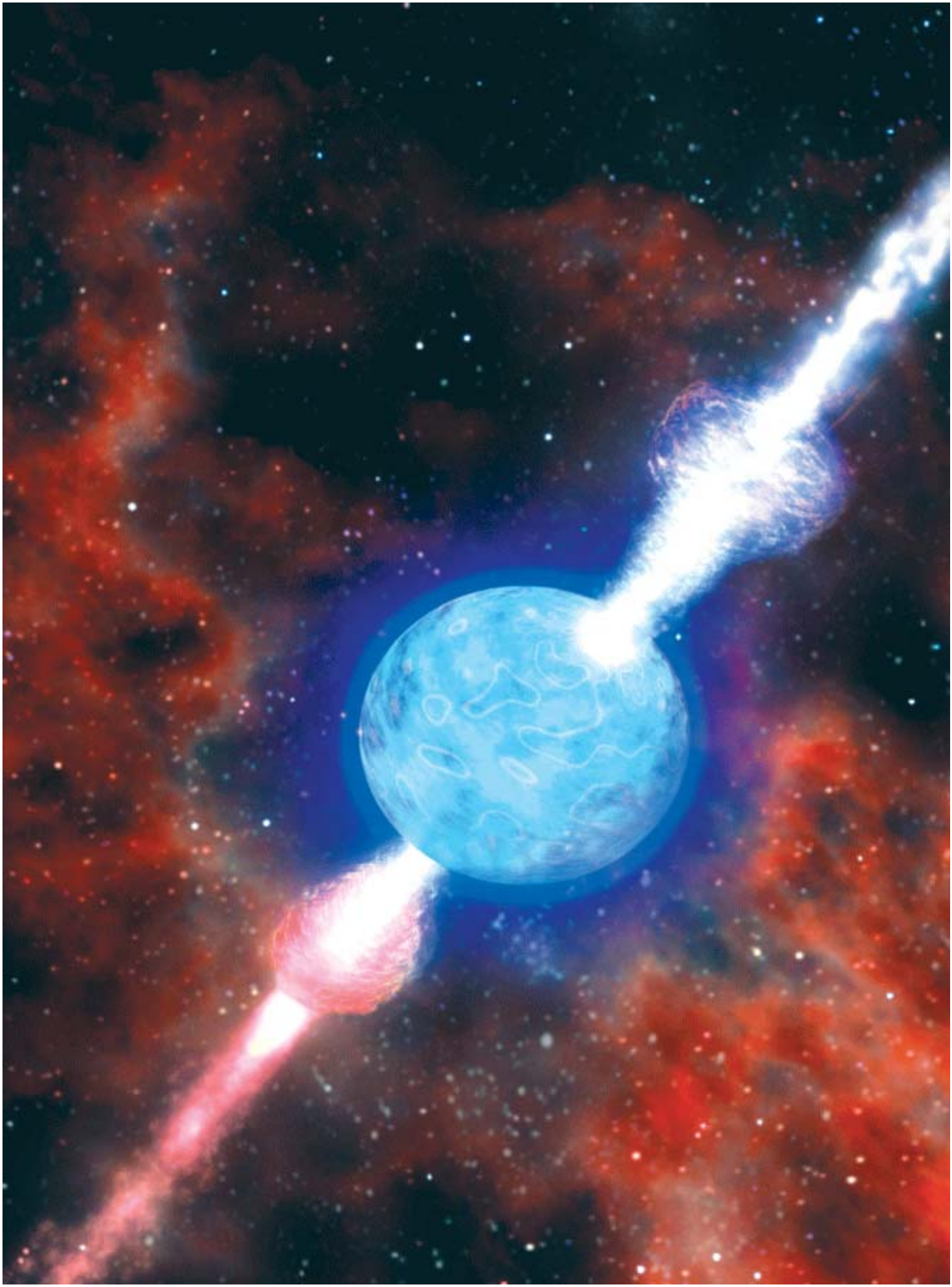

HI tidal tails, bridges and Clouds

B. S. Koribalski (ATNF)

Neutral hydrogen gas (HI) is abundant in most galaxies, but it is also found well outside their stellar envelopes where it contributes to the intergalactic medium. Prominent nearby examples of intergalactic gas include the Magellanic Stream and extended HI bridges in the M81 group of galaxies.

Koribalski and her collaborators are using observations taken with the Compact Array to study the HI gas found in the outskirts of galaxies and between galaxies. The data are being used to investigate how HI may be stripped by tidal forces from the parent galaxies into the intergalactic medium and how much HI is present in intergalactic gas. The smooth, extended HI disks seen in normal spiral galaxies are dynamically very different from other extended HI distributions. Galaxies with HI tails/plumes are generally peculiar and the location and kinematics of their outer HI component are shaped by galaxy collisons, mergers or tidal interactions.

One of the best resources for seeing the peculiar HI distributions in galaxies is the "HI Rogues' Gallery" compiled by Hibbard et al. (ASP Conf. Ser., 240, 659, 2001). This collection of images shows extended gas envelopes around some normal and peculiar galaxies, tidal tails/bridges in interacting or merging galaxy systems, large-scale rings around early type galaxies, and detached clouds at varying distances from associated galaxies.

Numerical simulations to study what happens to tidal debris over a long period of time have shown that a large fraction of the ejected HI gas will fall back onto the parent galaxy. The closest material falls back fastest, while more distant debris returns more slowly to accrete at larger distances from the galaxy centre. The simulations show that there is sufficient time for the slowly-returning material and any escaped gas to form bound entities and, potentially, stars. Some of these star-forming clumps may build new galaxies, such as tidal dwarf galaxies.

Some galaxies have very large HI envelopes extending way beyond their stellar distribution. The extended gas distributions show many different structures ranging from smooth disks to chaotic extensions. Because of their large extent, the outer neutral hydrogen disks are much more affected by tidal interactions than the stellar disks and are therefore an excellent tracer of the tidal forces. Collisions of galaxies with extended HI envelopes lead to large HI extensions, tails and bridges which can be found out to large distances from the galaxy centre. Recycling and re-accretion of these distant debris are important for the evolution of these systems.

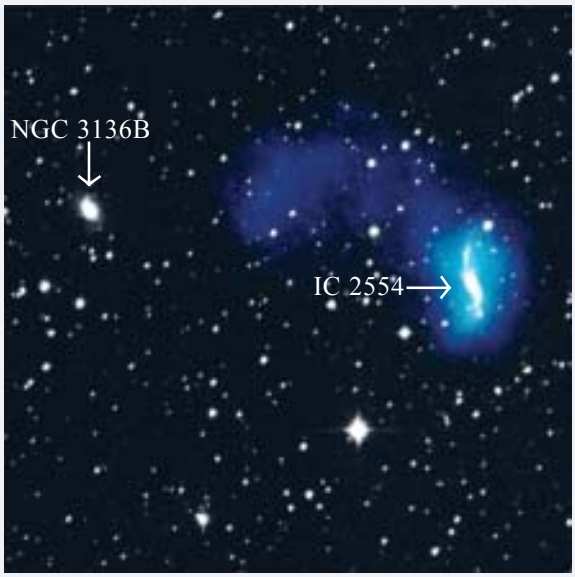

Figure 23 A Compact Array image showing the HI distribution (blue) towards the spiral galaxy IC 2554, shown overlaid on a 2MASS near-infrared (K-band) image. The large, one-sided HI plume emanating from IC 2554 possibly results from tidal interactions with a massive, elliptical galaxy NGC 3136B which is located approximately eight arcminutes to the east.
Image credit: B. Koribalski (ATNF), S. Gordon (UQld) and K. Jones (UQld).

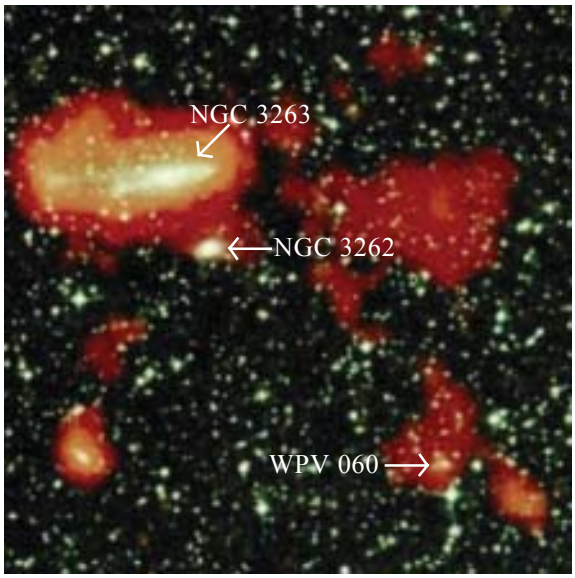

Figure 24 A Compact Array image of HI distribution (red) towards the peculiar galaxy NGC 3263, shown overlaid on a Digitized Sky Survey optical image. The spectacular HI plume to the west and south-west of NGC 3263/2 extends over approximately 175 x 200 kiloparsecs. The dwarf galaxy WPV 060 coincides with a peak in the southwest of the HI plume.
Image credit: J. English (UManit), B. Koribalski (ATNF) and K. Freeman (RSAA).

Figures 23 – 25 show Compact Array images that illustrate some excellent examples of peculiar and/or interacting galaxies. These have extended HI bridges or plumes that do not appear to have any stellar content. Figure 23 shows a one-sided, diffuse HI cloud near the peculiar spiral galaxy IC 2554 which lies at a distance of approximately 16 million parsecs from the Milky Way. The prominent plume emerging to the east of this galaxy is possibly caused by an interaction with the massive elliptical galaxy NGC 3136B. The plume has an extent of about 30 kiloparsecs and contains about a third of the total HI mass of the system (2 x 10^9 solar masses).

Figure 24 shows the HI distribution towards the peculiar spiral galaxy NGC 3263. This is a member of the NGC 3256 galaxy group at a distance of 37.6 million parsecs. Extended HI emission is seen around the galaxy itself, while a spectacular HI cloud of size approximately 175 x 100 kiloparsecs is seen to the west (right) of the galaxy. This cloud has an HI mass of approximately 10^9 solar masses. The dwarf galaxy WPV 060 which appears to be associated with an HI peak towards the south-western end of the cloud, could be a young galaxy formed out of the far-reaching tidal debris.

Detached HI clouds have been seen in many galaxy groups. These may constitute the gaseous material ejected furthest from the host galaxy and now disconnected from gas that has already returned. Figure 25 shows a spectacular example of this process. The HI distribution reveals a two-stranded bridge that spans the space between the galaxies NGC 6221 and NGC 6215, over a projected distance of nearly 100 kiloparsecs. The bridge has an HI mass of at least 1.4 x 10^8 solar masses. The NGC 6221/15 group also contains three HI-rich dwarf galaxies, one of which (Dwarf 3) is indicated in the inset of Figure 25.

The only intergalactic HI gas cloud detected in the HIPASS Bright Galaxy Catalog lies at a projected separation of 250 kiloparsecs from the galaxy NGC 2442 (distance = 15.5 Mpc) which is part of a loose group of galaxies. The cloud, HIPASS J0731-69, for which no optical counterpart has been detected, has an HI mass of 10^9 solar masses.

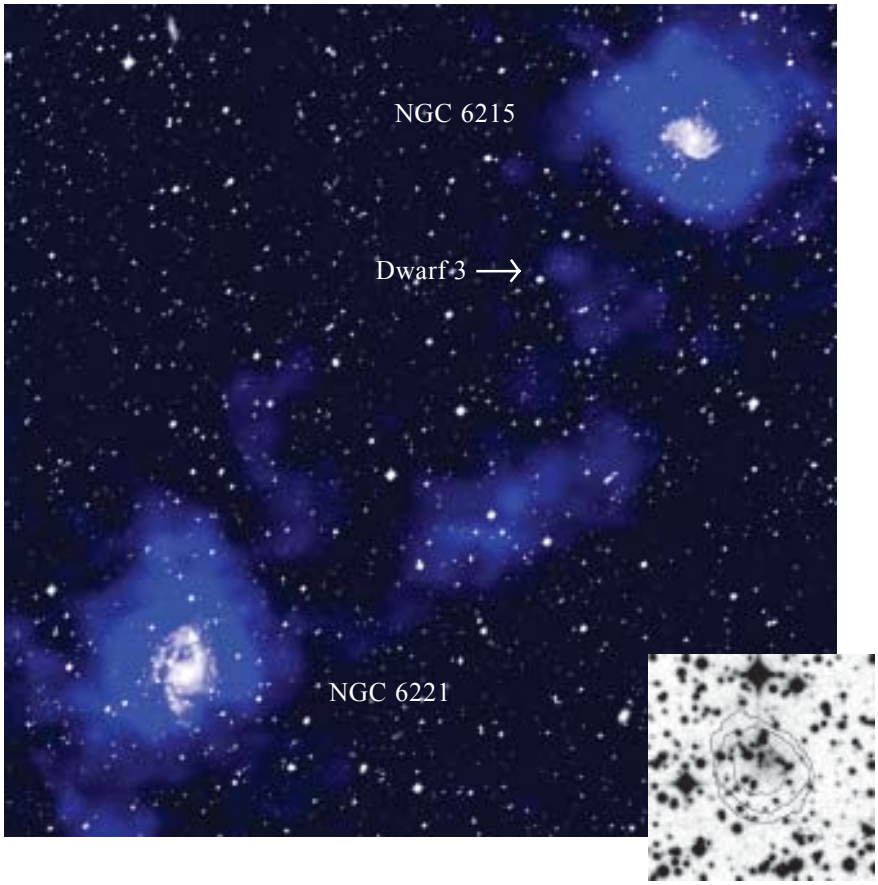

Figure 25 A Compact Array image of the HI distribution (blue) within a velocity range of 1490 to 1510 kilometres per second towards the interacting spiral galaxies NGC 6221 and NGC 6215 overlaid on a Digitized Sky Survey optical image. The narrow velocity range was chosen to emphasise a faint two-stranded HI bridge which probably resulted from NGC 6215 colliding with the outer HI disk of NGC 6221. The inset at the bottom right shows a close-up of Dwarf 3 which may have formed out of the debris.
Image credit: B. Koribalski (ATNF) and J. Dickey (UMinn).